cw Nonlinear Optics in Droplet Microcavities Displaying Enhanced Gain

H.-B. Lin and A. J. Campillo
Naval Research Laboratory, Optical Physics Branch, Code 5610, Washington, D.C. 20375-5338
(Received 20 August 1993)

A variety of stimulated nonlinear optical processes are observed under relatively low intensity cw excitation in droplet spherical microcavities. These include stimulated Raman and Rayleigh-wing scattering as well as four-wave parametric oscillation. The low thresholds for these stimulated processes are accounted for by all waves being in resonance with high-Q droplet modes and by the existence of a significant cavity QED enhancement (>100 times) in the nonlinear gain coefficients.

PACS numbers: 42.50.Wm, 12.20.Fv, 32.80.−t, 42.65.−k

There has been considerable interest recently in studies of optical resonators having dimensions comparable to the wavelength of light [1]. These can be used to fabricate very low threshold microlasers and to observe interesting quantum optical behavior. For example, when atoms are placed in a microcavity, radiative rates may be enhanced [2,3] (or inhibited [4]) by tuning the cavity resonance onto (or off) the emission frequency. Early demonstrations of cavity quantum electrodynamic (QED) modification at visible wavelengths utilized one-dimensional Fabry-Pérot cavities [5–8]. Recently, dramatic cavity QED effects have been observed in microdroplets [9–14]. Spontaneous emission from droplets show intense spectral peaks superimposed on the normal bulk emission [9] as well as modified fluorescence lifetimes [11] and enhanced lasing [12] and Raman gains [13]. Transparent droplets act as natural high-Q microresonators with feedback provided by whispering-gallery light waves [10,15]. A spherical cavity represents a case of three-dimensional confinement with large mode density enhancements ($>10^4$ times) [10] on resonance and cavity Q's as high as 2×10^8 [14] in the visible. In this Letter, we observe that a variety of third order nonlinear optical effects, normally seen in bulk liquids only under intense nanosecond pulse excitation, are readily duplicated using low power cw beams in droplets. For example, we observed continuous wave stimulated Raman scattering (SRS) with as little as 30 W/cm^2 incident excitation (corresponding to only three photons of laser pump in a cavity mode), four-wave parametric oscillation, and stimulated Rayleigh-wing scattering (SRWS) with Stokes shifts as great as 600 cm^{-1} at incident intensities of only 80 kW/cm^2. We attribute the low pump power requirements to all interacting waves being simultaneously resonant with high-Q droplet modes and by the presence of a significant cavity QED enhancement in nonlinear gain (gains 100× that normally observed in a bulk liquid).

Monodisperse streams of carbon disulfide droplets varying in size from 8 to 10, 12 to 15, 16 to 20, 24 to 30, and 32 to 40 μm in diameter were produced using a vibrating-orifice droplet generator [16] with nominal 5, 7.5, 10, 15, and 20 μm diameter orifices, respectively. Fine tuning of droplet size in each range was accomplished by varying the orifice frequency. Droplets were excited as they fell through a vertically polarized 514.5 nm cw argon-ion laser beam focused to a 40 μm spot diameter. Spectral composition of the scattered radiation was examined with (1) a scanning Spex 1 m double monochrometer (resolution of ca. 2.25 cm^{-1}) equipped with a cooled photomultiplier–photon-counting system, and (2) a lower resolution (ca. 10 cm^{-1}) $\frac{1}{3}$ m J-Y spectrograph equipped with a 1800 groove/mm grating and interfaced to a Princeton Instruments linear diode array detector. The higher sensitivity photon-counting system was used to examine *spontaneous* processes whereas the reduced sensitivity of the diode array allowed observation of only intense *stimulated* processes. Specific sizes were located in which laser, Stokes, and all nonlinearly generated wavelengths coincided with high-Q droplet resonances.

Figure 1, obtained using the low sensitivity diode array detector, shows a typical stimulated inelastic scattering spectrum in the range 18 800 to 18 200 cm^{-1} from CS_2 droplets (radius $a \approx 4.1$ μm) obtained with 1 W of laser power. The intense feature at 18 780 cm^{-1}, shifted 654 cm^{-1} to the red of the laser pump, is due to SRS associated with the C-S stretch vibrational model. This Stokes feature begins to grow nonlinearly at incident pump powers as low as 200 μW (30 W/cm^2). Although theory predicts the existence of cavity modes with very high Q's ($>10^{10}$) in droplets of this size, the highest values are limited by the large Rayleigh scattering losses, 10^{-3} cm^{-1} [17] in liquid CS_2, to a value of 10^8. Simultaneous cavity resonances at pump and Raman wavelengths lead to enhanced intracavity pump intensities and long effective interaction lengths. For example, a Q of 10^8 at the Raman wavelength leads to an effective path length ($\approx \lambda Q/2\pi n$, where n is the index of refraction) of ca. 5 m. Intracavity pump intensity, estimated [13] by multiplying the fraction of pump coupled into the resonance ($\approx \nu Q^{-1} \delta \nu_l^{-1}$, where $\delta \nu_l \approx 0.3$ cm^{-1} is the laser bandwidth) by the cavity buildup factor ($nQ/[2\pi a \nu]^2$), is about 100 times that of the incident intensity for modes having Q's in the range 10^5 to 10^8 under experimental conditions of Fig. 1. Us-

 0031-9007/94/73(18)/2440(4)$06.00 © 1994 The American Physical Society

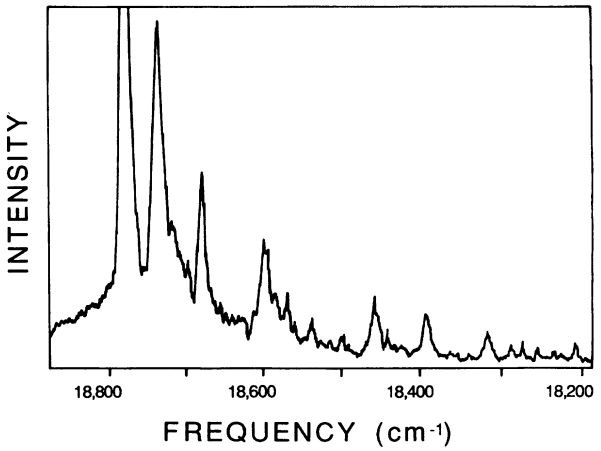

FIG. 1. Spectrum showing stimulated Rayleigh-wing scattering in 4.1 μm radius carbon disulfide microdroplets. The line at 18 780 cm^{-1} is the 654 cm^{-1} (symmetric C-S stretch) Raman Stokes of the cw 514.5 nm laser source which acts as a pump to drive SRWS features up to 600 cm^{-1} to the red. The positions of the specific SWRS lines correspond to available high-Q spherical cavity resonances of this size droplet. Peak amplitudes follow the theoretical asymptotic $\Delta\nu^{-1}$ dependence of stimulated Rayleigh-wing gain.

ing the estimated droplet enhanced pump intensity and effective path length and comparing our data to long-path experiments performed in liquid-core fibers [18] and to estimates based on published bulk liquid Raman gain [19], we find that our experimental droplet Raman threshold is at least a factor of 100 smaller than expected assuming bulk liquid behavior. This is consistent, however, with SRS droplet thresholds reported previously [13] and can be attributed to a cavity QED enhanced (100×) Raman gain coefficient of >2 cm/MW (compared to a bulk CS_2 value of 20 cm/GW). Note that in 4.1 μm radius droplets, the resonant pump threshold intensity of only 3 kW/cm^2 inside the droplet corresponds to as few as three green pump photons in the minimum volume azimuthal mode [20]. In order to clarify the role of QED gain enhancement in these experiments, we measured the SRS thresholds as a function of droplet size. Here the total gain is assumed equal to a gain coefficient g_c multiplied by the intracavity pump intensity I_c. Threshold for oscillation occurs when gain per length exceeds cavity loss per length, i.e., $g_c I_c > 2\pi n/\lambda Q$. Thresholds of 200 μW, 1 mW, 3 mW, 20 mW, and 45 mW were observed for nominal diameters of 8, 12, 16, 25, and 32 μm, respectively. The threshold follows an a^4 relationship ($g_c I_c \propto a^{-4}$). A portion of the variation in $g_c I_c$ is attributed to an a^{-2} dependence of I_c (assuming equal incident intensity) [21]. The remaining a^{-2} dependence can be attributed to cavity QED enhancement of g_c.

The familiar "Purcell formula" ($\eta = 3Q\lambda^3/4\pi^2 V_m$; V_m is cavity mode volume) [2] for cavity QED enhancement η, derived using Fermi's golden rule and the peak mode density at the center of the cavity resonance, is not applicable in liquid droplets [11] when the cavity mode width ($\delta\nu_c = \nu/Q$) becomes narrower than the homogeneous linewidth Γ of the nonlinear scattering process. In such a case, the *total* emission rate or scattering cross section will be averaged over regions of enhancement and inhibition. However, the functional dependence may be approximated by modifying Purcell's formula by substituting an equivalent material quality factor Q_m ($=\nu/\Gamma$). When this is done, the resulting functional form ($\eta \approx 3\lambda^2/4\pi^2\Gamma V_m$) is consistent with our observed size dependence since $1/V_m \propto a^{-2}$ [20]. This procedure, however, does not yield a good estimate of the magnitude of the gain enhancement because Purcell's η represents the ratio of the spontaneous rate of a single microcavity mode to the *total* spontaneous rate of all available free-space modes. Stimulated processes are inherently single mode effects. It is necessary to define a cavity gain coefficient enhancement κ which is obtained by dividing the spontaneous rate of a single microcavity mode by the spontaneous rate of a *single* mode of a macroscopic (or free-space) cavity. Performing such a calculation for spherical geometries under the assumption of broad Γ requires extensive numerical analysis and does not lead to a simple analytical expression. We present instead an approximation that treats the droplet as a simple Fabry-Pérot and yields an order of magnitude gain enhancement estimate. Following the procedure outlined in Ref. [8], the single mode enhancement is simply

$$\kappa = g_c/g_0 = \int_0^\infty \rho_c(\nu)R(\nu)\delta\nu \Big/ \int_0^\infty \rho_0(\nu)R(\nu)\delta\nu .$$

$R(\nu)$ is the square of the matrix element of the interaction Hamiltonian between the initial and final states and may be separated into frequency-dependent and -independent parts, $R_0 g_L(\nu,\Gamma)$, where $g_L(\nu,\Gamma)$ is a normalized Lorentzian line shape, $(\Gamma/2\pi)[(\nu-\nu_0)^2 + (\Gamma/2)^2]^{-1}$. The density of states per unit volume ρ_c (ρ_0) of the microcavity (large cavity) is calculated by counting only those modes having their k vectors perpendicular to the mirrors and leads to $\rho_c(\nu) = (1/V_m)g_L(\nu,\delta\nu_c) = (1/AL)g_L(\nu,\delta\nu_c)$ and $\rho_0 = 2/A$, where A is the mode cross sectional area and L is the cavity spacing. Integration under the assumption of $\delta\nu_c \ll \Gamma$ yields $\kappa \approx 2\Delta\nu_c/\pi\Gamma$ at line center, where $\Delta\nu_c$ is the frequency spacing between cavity modes ($\Delta\nu_c \approx 1/2L$). While this simple expression does not give the correct size dependence (the actual droplet calculation must include the effect of a slight spread in k vector directions that increases as droplet size decreases), it does demonstrate that significant gain enhancement is expected in 4.1 μm radius CS_2 droplets ($\kappa \approx 2\Delta\nu_c/\pi\Gamma \approx 350$ under conditions of Fig. 1; i.e., $\Delta\nu_c \approx 275$ cm^{-1} and $\Gamma = 0.5$ cm^{-1} for the 654 cm^{-1} Raman line).

At higher laser powers, the SRS Stokes wave, in turn, begins to act as a secondary pump and subsequently generates several types of nonlinear waves. For example, in Fig. 1 there are a series of stimulated features extending 600 cm^{-1} beyond the first Stokes toward the red. Similar superbroadened stimulated Rayleigh-wing scattering have been observed in bulk liquids [19,22] as well as in CS_2 liquid-core fibers [23] under intense nsec or psec excitation and are attributed to field induced molecular orientational motion. The greater internal intensity of the pump compared to nearby SRWS features enables us to rule out sequential multiorder Stokes SRWS generation to explain the superbroadening. Here also, the magnitude of the nonlinear optical gain appears greatly enhanced relative to the bulk value of 3 cm/GW [19]. Even though all relevant waves are near resonant in a high-Q cavity, there is not enough bulk SRWS gain present to allow such far-flung features at these experimental pump intensities. For example, superbroadening experiments in CS_2 liquid-core fibers [23], having comparable interaction lengths to our droplets, require over 2 orders of magnitude higher pump intensities even when the cavity effects of pump intensity resonant buildup are considered. This experimental number ($\kappa > 100$; see calculation [24]) is consistent with an estimate of $\kappa \approx 54$ using the $2\Delta\nu_c/\pi\Gamma$ approximation ($\Gamma = 3.2$ cm^{-1}) for the SRWS process.

Figure 2 shows scattering near the first SRS Stokes (here ν_1) for 4.4 μm radius droplets obtained with the high sensitivity photon-counting system. Argon-ion laser power of 50 mW was used. A second line, designated ν_2, has exceeded SRWS threshold. The three sets of features designated by ν_3's and ν_4's are due to the *spontaneous* parametric mixing process, $\nu_1 + \nu_2 \rightarrow \nu_3 + \nu_4$, via the induced nonlinear polarizations, $P_{3+i} = \chi^{(3)}E_1E_2E_{4-i}$. Here $i = 1$ or 0 and the E's are the electric fields at the corresponding optical frequencies. While a continuous range of ν_3, ν_4 frequencies satisfy the relation $\nu_1 + \nu_2 = \nu_3 + \nu_4$ and are nominally observed in high intensity bulk experiments [23], only those sets of discrete ν_3, ν_4 satisfying energy conservation and simultaneously in resonance with the droplet lead to peaks in the low intensity microdroplet case. In these cases, the anti-Stokes and Stokes waves are coupled [22]. The two peaks near 18 750 cm^{-1}, however, correspond to spontaneous Rayleigh-wing scattering with the Stokes wave decoupled from the anti-Stokes [22] (note resonance missing at ν_4). The rapid decrease in scattered peak heights ($\propto \Delta\nu^{-2}$) is consistent with a molecular orientational *spontaneous* scattering process (i.e., the classical Kerr nonlinearity). *The presence of such spontaneous peaks is a distinguishing feature of cavity QED.* The greater number of resonances here than in Fig. 1 (note the scale change) is explained by the appearance of lower-Q modes as well as the previously observed high-Q modes. All modes are expected to be visible in cavity QED *spontaneous* processes but not necessarily in stimulated scattering where the oscillation condition requires high Q. The similarity in apparent mode amplitudes when true peak heights are unresolved follows from the cavity QED enhancement per frequency being proportional to Q and the spectral widths being proportional to $1/Q$, leading to a spectrally integrated line intensity independent of mode order and cavity Q.

Figure 3, obtained with the low sensitivity diode array, shows droplets shifted slightly in size from that of Fig. 2 to allow higher-Q modes to participate in the parametric mixing. When the laser power was increased to 300 mW, four-photon parametric oscillation occurred (see stimulated anti-Stokes features near 18 800 cm^{-1}). The spectral range of Fig. 3 was expanded to illustrate the diversity of nonlinear processes encountered. Near 18 260 cm^{-1},

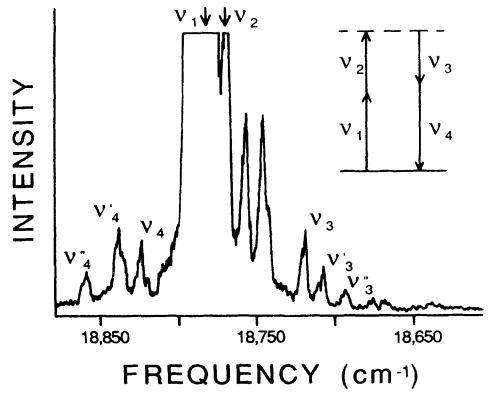

FIG. 2. Spectrum showing spontaneous four-wave parametric scattering in 4.4 μm radius CS_2 droplets. The waves at frequencies ν_1 and ν_2 are scattered into radiation at ν_3 and ν_4 as shown in the energy scheme outlined in the upper right-hand energy diagram.

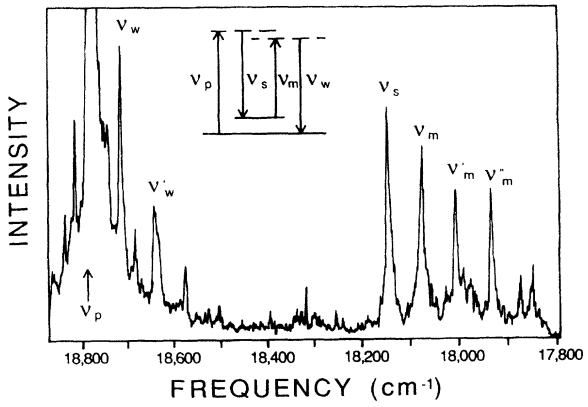

FIG. 3. Spectrum from 4.4 μm radius CS_2 droplets showing several nonlinear optical processes pumped by the wave at ν_p. The two anti-Stokes features at the extreme left are associated with four-photon parametric oscillation. Raman assisted biharmonic pumped four-wave difference frequency generation as outlined in the energy diagram at top center is evident between 17 800 and 18 200 cm^{-1}.

the presence of a second 654 cm^{-1} Stokes line is apparent. The three nearly equal intensity features to the red at intervals of 70–80 cm^{-1} are due to a biharmonic pumping process [25] as illustrated in the energy level diagram at the top center of Fig. 3 (i.e., $\nu_p + \nu_m \rightarrow \nu_w + \nu_s$, with ν_p, ν_w, ν_s, and ν_m associated with the spectral features indicated). It is clear from these initial studies that the cavity QED enhanced nonlinear optics of microspheres is extremely rich and warrants further theoretical and experimental investigation.

[1] Y. Yamamoto and R. E. Slusher, Phys. Today, **46**, No. 6, 66 (1993).

[2] E. M. Purcell, Phys. Rev. **69**, 681 (1946).

[3] P. Stehle, Phys. Rev. A **2**, 102 (1973); P. Goy, J. M. Raimond, M. Gross, and S. Haroche, Phys. Rev. Lett. **50**, 1903 (1983).

[4] D. Kleppner, Phys. Rev. Lett. **47**, 233 (1981); R. G. Hulet, E. S. Hilfer, and D. Kleppner, Phys. Rev. Lett. **55**, 2137 (1985).

[5] F. De Martini, G. Innocenti, G. Jacobovitz, and P. Mataloni, Phys. Rev. Lett. **59**, 2955 (1987); F. De Martini, M. Marrocco, P. Mataloni, and L. Crescentini, Phys. Rev. A **43**, 2480 (1991).

[6] H. Yokoyama, K. Nishi, T. Anan, H. Yamada, S. D. Brorson, and E. P. Ippen, Appl. Phys. Lett. **57**, 2814 (1990).

[7] D. J. Heinzen, J. J. Childs, J. E. Thomas, and M. S. Feld, Phys. Rev. Lett. **58**, 1320 (1987).

[8] H. Yokoyama and S. D. Brorson, J. Appl. Phys. **66**, 4801 (1989).

[9] R. E. Benner, P. W. Barber, J. F. Owen, and R. K. Chang, Phys. Rev. Lett. **44**, 475 (1980).

[10] S. C. Ching, H. M. Lai, and K. Young, J. Opt. Soc. Am. B **4**, 1995 (1987); **4**, 2004 (1987).

[11] H-B. Lin, J. D. Eversole, C. D. Merritt, and A. J. Campillo, Phys. Rev. A **45**, 6756 (1992).

[12] A. J. Campillo, J. D. Eversole, and H-B. Lin, Phys. Rev. Lett. **67**, 437 (1991).

[13] H-B. Lin, J. D. Eversole, and A. J. Campillo, Opt. Lett. **17**, 828 (1992).

[14] P. Chylek, H-B. Lin, J. D. Eversole, and A. J. Campillo, Opt. Lett. **16**, 1723 (1991).

[15] S. C. Hill and R. E. Benner, in *Optical Effects Associated with Small Particles,* edited by P. W. Barber and R. K. Chang (World Scientific, Singapore, 1988), Chap. 1, pp. 3–61.

[16] H-B. Lin, J. D. Eversole, and A. J. Campillo, Rev. Sci. Instrum. **61**, 1018 (1990).

[17] J. Stone, J. Opt. Soc. Am. **62**, 327 (1972).

[18] J. Stone, Appl. Phys. Lett. **26**, 163 (1975).

[19] W. Kaiser and M. Maier, in *Laser Handbook,* edited by F. T. Arecchi and E. O. Schulz-Dubois (North-Holland, Amsterdam, 1972), Vol. 2, p. 1077.

[20] V. B. Braginsky, M. L. Gorodetsky, and V. S. Ilchenko, Phys. Lett. A **137**, 393 (1989).

[21] C. C. Lam, P. T. Leung, and K. Young, J. Opt. Soc. Am. B **9**, 1585 (1992).

[22] R. Y. Chiao, P. L. Kelley, and E. Garmire, Phys. Rev. Lett. **17**, 1158 (1966).

[23] G. S. He and P. N. Prasad, Phys. Rev. A **41**, 2687 (1990).

[24] The fraction of 514.5 nm laser power overlapping a high-Q ($>10^5$) cavity resonance is the ratio of their respective spectral widths ($\nu Q^{-1} \delta\nu_l^{-1}$). The intensity of laser light within the droplet is estimated from Eq. (4.15) of Ref. [21] multiplied by $\nu Q^{-1} \delta\nu_l^{-1}$ and is independent of cavity Q but dependent on the laser bandwidth ($\delta\nu_l = 0.3$ cm^{-1}). A measured 0.1 W (16 kW/cm^2) threshold for the SRWS feature at $\Delta\nu \approx 390$ cm^{-1} corresponds to an estimated I_c of 3.2 MW/cm^2. The fraction of 514.5 nm radiation converted to SRS pump is estimated at 33% [19] for high intensities. The requirement that the gain per unit length exceed the losses per unit length for cavity oscillation may be written $g_c > 2\pi n / f I_p \lambda Q$. Here f is a factor reflecting the spatial overlap efficiency between the pump and SRWS modes, which are of different orders [15]. Using a value of $f \approx 0.25$ calculated using Lorenz-Mie theory and a $Q \approx 10^8$, limited by measured [17] internal scattering in the liquid, we obtain $g_c > 7.2$ cm/GW. However, assuming a gain of the form $\Delta\nu/(\Gamma^2 + \Delta\nu^2)$ and a peak bulk gain coefficient of 3 cm/GW [21], the bulk gain at 390 cm^{-1} is only 0.05 cm/GW. Therefore, experimental results are consistent with $\kappa > 144$.

[25] D. C. Hanna, M. A. Yuratich, and D. Cotter, *Nonlinear Optics of Free Atoms and Molecules*(Springer-Verlag, New York, 1979).